



1

One hundred ways to process time, frequency, rate and scale in the auditory cortex: a pattern-recognition meta-analysis

Edgar Hemery^{1,*}, Jean-Julien Aucouturier^{2,*}

¹Centre de Robotique (CAOR), École Nationale Supérieure des Mines de Paris, Paris, France

²Science et Technologie de la Musique et du Son (STMS), IRCAM/CNRS UMR9912/UPMC, Paris, France

Correspondence*:

JJ Aucouturier

IRCAM, 1 Place Stravinsky, 75004 Paris, France, aucouturier@gmail.com

2 ABSTRACT

3 The mammalian auditory system extracts features from the acoustic environment based on the
4 responses of spatially distributed sets of neurons in the subcortical and primary cortical audi-
5 tory structures. The characteristic responses of these neurons (linearly approximated by their
6 spectro-temporal receptive fields, or STRFs) suggest that auditory representations are formed
7 on the basis of a time, frequency, rate (temporal modulations) and scale (spectral modulati-
8 ons) analysis of sound. However, how these four dimensions are integrated and processed in
9 subsequent neural networks remains unclear. In this work, we present a new methodology to
10 generate computational insights into the functional organization of such processes. We first pro-
11 pose a systematic framework to explore more than a hundred different computational strategies
12 to process the output of a generic STRF model. We then evaluate these strategies on their abi-
13 lity to compute perceptual distances between pairs of environmental sounds. Finally, we conduct
14 a meta-analysis of the dataset of all these algorithms' accuracies to examine whether certain
15 combinations of dimensions and certain ways to treat such dimensions are, on the whole, more
16 computationally effective than others. We present an application of this methodology to a dataset
17 of ten environmental sound categories, in which the analysis reveals that (1) models are most
18 effective when they organize STRF data into frequency groupings - which is consistent with the
19 known tonotopic organisation of receptive fields in A1 -, and that (2) models that treat STRF
20 data as time series are no more effective than models that rely only on summary statistics along
21 time - which corroborates recent experimental evidence on texture discrimination by summary
22 statistics.

23 **Keywords:** Spectro-temporal receptive fields; auditory cortex; audio pattern recognition

1 INTRODUCTION

24 The mammalian auditory system extracts features from the acoustic environment based on the responses
25 of spatially distributed sets of neurons in the primary auditory cortex (A1). These neurons operate on the
26 preprocessing done by subcortical structures such as the inferior colliculus, and the auditory periphery.
27 Their behaviour can be modelled as a spectro-temporal filterbank, in which the transformation between
28 the sound input and the firing-rate output of each neuron is approximated linearly by its spectro-temporal

29 receptive field (STRF)(**Chi et al.**, 2005). An auditory neuron's STRF can be described as a 2-dimensional
30 filter in the space of spectro-temporal modulations, with a bandwidth in the two dimensions of rate (tem-
31 poral modulation, in Hz) and scale (spectral modulation, in cycles/octave). In addition, because auditory
32 cortical neurons are tonotopically organized and respond to frequency-specific afferents, a given neuron's
33 STRF only operates on a specific frequency band. The convolution between the rate-scale STRF and the
34 time-frequency spectrogram of the sound gives an estimate of the time-varying firing rate of the neuron
35 (Figure 1).

36 Although the experimental measurement of A1 STRFs in live biological systems is plagued with meth-
37 odological difficulties (**Christianson et al.**, 2008), and their approximation of the non-linear dynamics
38 and context-dependency of auditory cortical neurons is only partial (**Gourévitch et al.**, 2009), computa-
39 tional simulations of even simple STRFs appear to provide a robust model of the representational space
40 embodied by the auditory cortex. **Patil et al.** (2012) have recently demonstrated a system which uses a
41 Gabor-filter implementation of STRFs to compute perceptual similarities between short musical tones. In
42 their implementation, sound signals were represented as the mean output energy in time of a bank of more
43 than 30,000 neurons, evenly spaced according to their characteristic frequencies, rates and scales. This
44 high-dimensional representation was then reduced using principal component analysis, and used to train a
45 gaussian-kernel distance function between pairs of sounds. The authors found that their model approxima-
46 tes psychoacoustical dissimilarity judgements made by humans between pairs of sounds to near-perfect
47 accuracy, and better so than alternative models based on simpler spectrogram representation.

48 Such computational studies (see also **Fishbach et al.** (2003)) provide proofs that a given combination of
49 dimensions (e.g. frequency/rate/scale for **Patil et al.** (2012); frequency/rate for **Fishbach et al.** (2003)),
50 and a given processing applied on it, is sufficient to give good performance; they do not, however, answer
51 the more general questions of what combination of dimensions is optimal for a task, in what order these
52 dimensions are to be integrated, or whether certain dimensions are best summarized rather than treated
53 as an orderly sequence. In other words, while it seems plausible that cognitive representations are formed
54 on the basis of a time, frequency, rate and scale analysis of auditory stimuli, and while much is known
55 about how A1 neurons encode such instantaneous sound characteristics, how these four dimensions are
56 integrated and processed in subsequent neural networks remains unclear.

57 Human psychophysics and animal neurophysiology have recently cast new light on some of these sub-
58 sequent processes. First, psychoacoustical studies of temporal integration have revealed that at least part
59 of the human processing of sound textures relies only on temporal statistics, which do not retain the tem-
60 poral details of the feature sequences (**McDermott et al.**, 2013; **Nelken and de Cheveigné**, 2013). But
61 the extent to which this type of timeless processing generalizes to any type of auditory stimuli remains
62 unclear; similarly, the computational purpose of this type of representation is unresolved: does it e.g. pro-
63 vide a higher-level representational basis for recognition, or a more compact code for memory? Second,
64 a number of studies have explored contextual effects on activity in auditory neurons (e.g. **Ulanovsky**
65 **et al.** (2003), **David and Shamma** (2013)). These effects are evidence for how sounds are integrated over
66 time, and constrain their neural encoding (**Asari and Zador**, 2009). Finally, the neurophysiology of the
67 topological organization of auditory neuronal responses also provides indirect insights into the compu-
68 tational characteristics of the auditory system. For instance, it is well-established that several auditory
69 cortical areas show an orderly mapping of characteristic frequency (CF) in space: the tonotopical map
70 (**Eggermont**, 2010). This organization plausibly reflects a computational need to process several areas of
71 the frequency axis separately, as shown e.g. with frequency-categorized responses to natural meows in cat
72 cortices (**Gehr et al.**, 2000). However, the topology of characteristic responses in the dimensions of rate
73 and scale remains intriguing: while STRFs are orderly mapped in the auditory areas of the bird forebrain,
74 with clear layer organization of rate tuning (**Kim and Doupe**, 2011), no strong organization of STRF
75 shapes has been observed to date in the mammalian auditory cortex (**Atencio and Schreiner**, 2010) - but
76 it has in the midbrain (**Baumann et al.**, 2011). Conversely, if, in birds, scale gradients seem to be mapped
77 independently of tonotopy, in A1 they vary systematically within each isofrequency lamina (**Schreiner**
78 **et al.**, 2000). It is therefore plausible that the mammalian cortex has evolved networks able to jointly
79 process the time, frequency, rate and scale dimensions of auditory stimuli into a combined representations

80 optimized for perceptive tasks such as recognition, categorization and similarity. But there are many ways
81 to form such representations, and insights are lacking as to which are most effective or efficient.

82 This work presents a new computational approach to derive insights on what conjunct processing of the
83 4 dimensions of time, frequency, rate and scale makes sense at a cortical level. To do so, we propose a
84 systematic pattern-recognition framework to, first, design more than a hundred different computational
85 strategies to process the output of a generic STRF model; second, we evaluate each of these algorithms
86 on their ability to compute acoustic dissimilarities between pairs of sounds; third, we conduct a meta-
87 analysis of the dataset of these many algorithms' accuracies to examine whether certain combinations of
88 dimensions and certain ways to treat such dimensions are more computationally effective than others.

2 METHODS

2.1 OVERVIEW

89 Starting with the same STRF implementation as **Patil et al.** (2012), we propose a systematic framework
90 to design a large number of computational strategies (precisely: 108) to integrate the four dimensions
91 of time, frequency, rate and scale in order to compute perceptual dissimilarities between pairs of audio
92 signals.

93 As seen below (section 2.2), the STRF model used in this work operates on 128 characteristic frequen-
94 cies, 22 rates and 11 scales. It therefore transforms a single auditory spectrogram (dimension: $128 \times \text{time}$,
95 sampled at $\text{SR}=125\text{Hz}$) into $22 \times 11=242$ spectrograms corresponding to each of the 242 STRFs in the
96 model. Alternatively, its output can be considered as a series of values taken in a frequency-rate-scale
97 space of dimension $128 \times 22 \times 11=30,976$, measured at each successive time window.

98 The typical approach to handling such data in the field of audio pattern recognition, and in the Music
99 Information Retrieval (MIR) community in particular (**Orio**, 2006), is to represent audio data as a tem-
100 poral series of *features*, which are computed on successive temporal windows. Features are typically
101 seen as points in a corresponding vector space; the series of such feature points in time represents the
102 signal. Feature series can then be modelled and compared to one another with e.g. first-order statisti-
103 cal distributions (the so-called bag-of-frame approach of **Aucouturier and Pachet** (2007a)), dynamical
104 models (**Lagrange**, 2010), Markov models (**Flexer et al.**, 2005) or alignment distances (**Aucouturier**
105 **and Pachet**, 2007b). Taking inspiration from this approach, we construct here twenty-six models that
106 treat the dimension of time as a series that takes its values in various combinations of frequency, rate and
107 scale: for instance, one can compute a single scale vector (averaged over all frequencies and rates) at each
108 time window, then model the corresponding temporal series with a Gaussian mixture model (GMM), and
109 compare GMMs to one another to derive a measure of distance.

110 However, we propose here to generalize this approach to devise models that also take series in other
111 dimensions than time (see sections 2.3 and 2.4). For instance, one can consider values in rate/scale space
112 as successive steps in a frequency series (or, equivalently, successive "positions" on the frequency axis).
113 Such series can then be processed like a traditional time series, e.g. modelled with a gaussian mixture
114 model or compared with alignment distances. Using this logics, we can create twelve frequency-series
115 models, twelve rate-series models and twelve scale-series models. Many of these models have never
116 been considered before in the pattern recognition literature. Finally, we add to the list fourty four models
117 that do not treat any particular dimension as a series, but rather apply dimension reduction (namely,
118 PCA) on various combinations of time, frequency, rate and scale. For instance, one can average out the
119 time dimension, apply PCA on the frequency-rate-scale space, yielding a single high-dimensional vector
120 representation for each signal; vectors can then be compared with e.g. euclidean distance. One of these
121 'vector' models happens to be the approach of **Patil et al.** (2012); we compare it here with fourty-three
122 alternative models of the same kind.

123 We can then test each of these 108 models for their ability to match reference judgements on any given
124 dataset of sound stimuli. For instance, given a dataset of sound files organized in categories, each of
125 the models can be tested for its individual ability to retrieve, for any file, nearest neighbors that belong
126 to the same category (i.e. its *precision*). The better precision is achieved by a given model, the better
127 approximation to the actual biological processing it is taken to represent, at least for the specific dataset it
128 is being tested on.

129 Finally we conduct a meta-analysis of the set of 108 precision values achieved by the models. By
130 comparing precisions between very many models, each embedding a specific sub-representation based on
131 the STRF space, we can generate quantitative evidence of whether certain combinations of dimensions and
132 certain ways to treat such dimensions are, on the whole, more computationally effective than others for
133 that dataset of sounds. For instance, among the 106 models considered here, 16 operate only on frequency,
134 16 on frequency and rate, and 16 on frequency and scale ; if compared with inferential statistics, these 48
135 models provide data to examine whether there is a systematic, rather than incidental, advantage to one or
136 the other combination.

2.2 STRF IMPLEMENTATION

137 We use the STRF implementation of **Patil et al.** (2012), with the same parameters. The STRF model
138 simulates the cortical processing occurring in the auditory thalamus and cortex. It processes the output of
139 the cochlea - represented by an auditory spectrogram in log frequency (SR= 24 channels per octave) vs
140 time (SR=125Hz, 8ms time windows) using a multitude of STRFs centered on specific frequencies (128
141 channels, 5.3 octaves), rates (22 filters: +/-4.0, +/-5.8, +/-8.0, +/-11.3, +/-16.0, +/-22.6, +/-32.0, +/-45.3,
142 +/-64.0, +/-90.5, +/-128.0 Hz) and scales (11 filters: 0.25, 0.35, 0.50, 0.71, 1.0, 1.41, 2.00, 2.83, 4.00,
143 5.66, 8.00 c/o). (Figure 1-1)

144 Each time slice in the auditory spectrogram is Fourier-transformed with respect to the frequency axis
145 (SR=24 channels/octave), resulting in a cepstrum in scales (cycles per octave) (Figure 1-3). Each scale
146 slice is then Fourier-transformed with respect to the time axis (SR=125Hz), to obtain a frequency spectrum
147 in rate (Hz) (Figure 1-4). These two operations result in a spectrogram in scale (cycles/octave) vs rate
148 (Hz). Note that we keep all output frequencies of the second FFT, i.e. both negative rates from -SR/2
149 to 0 and positive rates from 0 to SR/2. Each STRF is a bandpass filter in the scale-rate space. First, we
150 filter in rate: each scale slice is multiplied by the rate-projection of the STRF, a bandpass-filter transfer
151 function H_r centered on a given cut-off rate (Figure 1-5). This operation is done for each STRF in the
152 model. Each band-passed scale slice is then inverse Fourier-transformed w.r.t. rate axis, resulting in a
153 scale (c/o) vs time (frames) representation (Figure 1-6). We then apply the second part of the STRF
154 by filtering in scale: each time slice is multiplied by the scale-projection of the STRF, a bandpass-filter
155 transfer function H_s centered on a given cut-off scale (Figure 1-7). This operation is done for each STRF
156 in the model. Each band-passed time slice is then inverse Fourier-transformed w.r.t. scale axis, returning
157 back to the original frequency (Hz) vs time (frames) representation (Figure 1-8). In this representation,
158 each frequency slice therefore corresponds to the output of a single cortical neuron, centered on a given
159 frequency on the tonotopic axis, and having a given STRF. The process is repeated for each STRF in the
160 model ($22 \times 11 = 242$).

2.3 DIMENSIONALITY REDUCTION

161 The STRF model provides a high-dimensional representation: $(128 \times 22 \times 11 = 30,976) \times$ time sampled
162 at SR=125Hz. Upon this representation, we construct more than a hundred algorithmic ways to compute
163 acoustic dissimilarities between pairs of audio signals. All these algorithms obey to a general pattern
164 recognition workflow consisting of a dimensionality reduction stage, followed by a distance calculation
165 stage (Figure 2). The dimensionality reduction stage aims to reduce the dimension ($d=30,976 \times$ time)
166 of the above STRF representation to make it more computationally suitable to the algorithms operating

167 in the distance calculation stage and/or to discard dimensions that are not relevant to compute acoustic
168 dissimilarities. Algorithms for dimensionality reduction can be either data-agnostic or data-driven.

169 1. Algorithms of the first type rely on reduction strategies that are independent of the statisti-
170 cal/informational properties of the specific data to which they are applied, but rather decided based
171 on a priori, generic intuitions. As a representative example of this type of approach, we use

172 • summary statistics, in which we collapse the original STRF representation by averaging out data
173 along one or several of its 4 physical dimensions. For instance, by averaging along time, we
174 reduce the original time-series in a feature space of $d=30,976$ to a single mean frame of size d :

$$STRF_T(f, r, s) = \frac{1}{N_T} \sum_{t=1}^{t=N_T} STRF(t, f, r, s), \forall f, r, s \quad (1)$$

175 where N_T is the number of measured time points in the original representation. By averaging
176 along frequency, we obtain a time-series of rate-scale maps of size $d=22 \times 11=242$:

$$STRF_F(t, r, s) = \frac{1}{N_F} \sum_{f=1}^{f=N_F} STRF(t, f, r, s), \forall t, r, s \quad (2)$$

177 where N_F is the number of measured frequency points in the original representation ($N_F = 128$).

178 2. Data-driven approaches to dimensionality reduction select or reorganize the dimensions of the data
179 based on the data's specific properties, often in the aim of optimizing a criteria such as its variability
180 or compactness. As a representative example of this approach, we use

181 • Principal Component Analysis (PCA), which finds optimal linear combinations of the data's ori-
182 ginal dimensions so as to account for as much of the variability in the data as possible, while
183 having fewer dimensions than the original. In order to compute data variability, PCA operates
184 on the complete dataset of audio signals used for the evaluation, and then applies the optimal
185 reduction rules on each individual signal. In this work, we implemented PCA using the fast tru-
186 ncated singular value decomposition (SVD) method (**Halko et al.**, 2011), and used it to reduce
187 the original number of dimensions to a variable number of principal components accounting for
188 a fixed variance threshold of 99.99% of the original variance.

189 As illustrated in Figure 2, the two types of approaches can be applied jointly, and on any combination
190 of dimensions. For instance, one can collapse the time dimension to create a single mean frame of size
191 $d=30,976$ (approach 1), then consider this collapsed data as a frequency-series (of 128 measured frequency
192 points) taking values in the rate-scale space ($d=242$) and apply PCA on this space to account for 99.99%
193 of the rate-scale variance (approach 2). The result is a frequency-series (of 128 points) taking its values in
194 a reduced feature space of dimension $d < 242$.

195 Table 1 lists the fifteen combinations of dimensions to which the original STRF representation can be
196 reduced. Some of these reduced representations correspond to signal representations that are well-known
197 in the audio pattern recognition community: for instance, by averaging over frequency, rate and scale,
198 the STRF representation is reduced to a time series of energy values, i.e. a waveform; by averaging only
199 over rate and scale, it is reduced to a spectrogram. More sophisticated combinations are also conceptually
200 similar to existing, if sometimes more obscure, proposals: by averaging over frequency and rate, STRF
201 can be viewed as a time series of scale values, which is reminiscent of the Mel-frequency cepstrum
202 coefficients that are prevalent in speech and music recognition (**Logan and Salomon**, 2001); time-rate
203 representations have been previously called "modulation spectrum" (**Peeters et al.**, 2002), and frequency-
204 rate representations "fluctuation patterns" (**Pampalk**, 2006). At the other extreme, a number of reduced

205 representations derived here from the STRF model are probably entirely original, albeit obeying to the
206 same combinatorial framework as their better known parents.

2.4 DISTANCE CALCULATION

207 Following dimensionality reduction, STRF representations are compared in order to compute acoustic
208 distances between pairs of audio signals. Distance calculation algorithms differ on whether they treat a
209 signal's STRF data as a single multidimensional point in a vector space, or as a series of points.

210 1. Algorithms treating STRF data as a single multidimensional point rely on distance functions operating
211 on the data's vector space. For the purpose of this work, we use two representative instances of such
212 functions:

213 • the simple euclidean distance, defined as

$$d_e(p, q) = \sqrt{\sum_i (p_i - q_i)^2} \quad (3)$$

214 where p_i and q_i are the i^{th} coordinate of points p and q , and.

215 • the gaussian kernel distance, which generalizes the approach of the euclidean distance by scaling
216 each dimension i separately with a weight σ_i optimized to match the reference distance matrix
217 we seek to obtain. It is computed as

$$d_K(p, q) = \exp\left(-\sum_i \frac{(p_i - q_i)^2}{\sigma_i^2}\right) \quad (4)$$

218 where the σ_i s are learned by gradient descent to minimize the difference between the calculated
219 $d_K(p, q)$ and the true $d(p, q) \forall p, q$, using the cost function given as:

$$J = -\frac{1}{n^2} \sum_p \sum_q (d(p, q) - \bar{d})(d_K(p, q) - \bar{d}_K) \quad (5)$$

220 where $d(p, q)$ is the true distance between p and q , \bar{d} is the mean distance over all (p, q) pairs,
221 $d_K(p, q)$ is the kernel distance between p and q and \bar{d}_K is the mean kernel distance over all
222 (p, q) pairs. We used the Matlab gradient descent implementation of Carl Edward Rasmussen and
223 Olivier Chappelle (<http://olivier.chapelle.cc/ams/>).

224 2. Algorithms treating STRF data as a series of points rely on distance functions able to operate either on
225 ordered data, or on unordered collections of points. As a representative instance of the first approach,
226 we use:

227 • the dynamic time warping (DTW) algorithm, $d_{DTW}(p, q)$, which is computed as the cost of
228 the best alignment found between the 2 series p and q , using the individual cosine distances
229 between all frames $p[n], n < \text{length}(p)$ and $q[m], m < \text{length}(p)$. Note that, if it is tradition-
230 nally used with time-series, the DTW algorithm can be applied regardless of whether series p
231 and q are ordered in time, or in any other dimension (we therefore also refer to it here by its
232 more generic name dynamic programming (DP)). We computed d_{DTW} using Dan Ellis' Matlab
233 implementation (<http://www.ee.columbia.edu/~dpwe/resources/matlab/dtw/>).

234 As a representative instance of the second approach, we use:

- 235 • Gaussian mixture models (GMM), compared with Kullback-Leibler divergence. A GMM is a
 236 statistical model to estimate a probability distribution $\mathcal{P}(x)$ as the weighted sum of M gaussian
 237 distributions $\mathcal{N}_i, \forall i < M$, each parameterized by a mean μ_i and covariance matrix Σ_i ,

$$\mathcal{P}(x) = \sum_i^M \pi_i \mathcal{N}_i(x, \mu_i, \Sigma_i) \quad (6)$$

238 where π_i is the weight of gaussian distribution \mathcal{N}_i . Given a collection of points, viewed as sam-
 239 ples from a random variable, the parameters $\pi_i, \mu_i, \Sigma_i, \forall i < M$ of a GMM that maximizes the
 240 likelihood of the data can be estimated by the E-M algorithm (Bishop and Nasrabadi, 2006).
 241 For this work, we take $M=3$. In order to compare two series p and q , we estimate the parameters
 242 of a GMM for each of collection of points $p[n]$ and $q[m]$, and then compare the two GMMs \mathcal{P}_p
 243 and \mathcal{P}_q using the Kullback Leibler (KL) divergence:

$$d_{KL}(p, q) = \int \mathcal{P}_p(x) \log \frac{\mathcal{P}_q(x)}{\mathcal{P}_p(x)} \quad (7)$$

244 computed with the Monte-Carlo estimation method of Aucouturier and Pachet (2004). Note
 245 that, similarly to DTW, if GMMs and KL divergence are traditionally used with time-series, they
 246 can be applied regardless of whether series p and q correspond to successive positions in time, or
 247 in any other dimension.

248 The choice to view data either as a single point or as a series is sometimes dictated by the physical
 249 dimensions preserved in the STRF representation after dimensionality reduction. If the time dimension is
 250 preserved, then data cannot be viewed as a single point because its dimensionality would then vary with
 251 the duration of the audio signal and we wouldn't be able to compare sounds to one another in the same
 252 feature space; it can only be processed as a time-series, taking its values in a constant-dimension feature
 253 space. For the same reason, series sampled in frequency, rate or scale cannot take their values in a feature
 254 space that incorporates time. The same constraint operates on the combination of dimensions that are
 255 submitted to PCA: PCA cannot reduce a feature space that incorporates time, because its dimensionality
 256 would not be constant. PCA can be applied, however, on the constant-dimension feature space of a time-
 257 series. Table 1 describes which modeling possibility applies to what combination of dimensions. The
 258 complete enumeration of all algorithmic possibilities yields 108 different models.

3 CASE STUDY: TEN CATEGORIES OF ENVIRONMENTAL SOUND TEXTURES

259 We present here an application of the methodology to a small dataset of environmental sounds. We com-
 260 pute precision values for 108 different algorithmic ways to compute acoustic dissimilarities between pairs
 261 of sounds of this dataset. We then analyse the set of precision scores of these algorithms to examine
 262 whether certain combinations of dimensions and certain ways to treat such dimensions are more com-
 263 putationally effective than others. We show that, even for this small dataset, this methodology is able
 264 to identify patterns that are relevant both to computational audio pattern recognition and to biological
 265 auditory systems.

3.1 CORPUS AND METHODS

266 One hundred 2-second audio files were extracted from field recordings contributions on the Freesound
 267 archive (<http://freesound.org>). For evaluation purpose, the dataset was organized into 10 categories of
 268 environmental sounds (*birds, bubbles, city at night, clapping door, harbour soundscape, inflight infor-*
 269 *mation, pebble, pouring water, waterways, waves*), with 10 sounds in each category. File formats were

270 standardized to mono, 44.1kHz, 16-bit, uncompressed, and RMS normalized. The dataset is available as
 271 an internet archive: <https://archive.org/details/OneHundredWays>.

272 On this dataset, we compare the performance of exactly 108 different algorithmic ways to compute
 273 acoustic dissimilarities between pairs of audio signals. All these algorithms are based on combinaisons
 274 of the four T,F,R,S dimensions of the STRF representation. To describe these combinations, we adopt the
 275 notation $X>A, B, \dots$ for a computational model based on a series in the dimension of X, taking its values in
 276 a feature space consisting of dimensions A, B, ... For instance, a time series of frequency values is written
 277 as $T>F$ and time series of any suitable feature space are written as $T>*$, where * is a wildcard character.
 278 In the following, PCA refers to *principal component analysis* (a data-driven dimensionality reduction
 279 method), GMM and KL to *gaussian mixture model* and *Kullback-Leibler divergence* resp. (a statistical
 280 distribution estimation method used to model series, and a distance measure used to compare models
 281 to one another), DP to *dynamic programming* (a method to compare series by computing the optimal
 282 alignment from one to the other), `KERNEL SC.` and `KERNEL` to *kernel scaling* and *kernel distance* resp.
 283 (the process of estimating optimal weights in a gaussian kernel distance with respect to a target set of
 284 dissimilarities, and the utilization of such weights to compute a distance between vectors) and `EUCL` to
 285 the *euclidean distance*. All these algorithms correspond to those described in section 2.

286 In order to compare the performance of the algorithms, we used the same evaluation methodology as
 287 earlier work about music similarity measures (Aucouturier and Pachet, 2004): each of the models is
 288 tested for its individual ability to retrieve, for any file, nearest neighbors that belong to the same category.
 289 More precisely, for a given algorithm and a given sound query in the dataset, a result is considered relevant
 290 if the retrieved sound belongs to the same category as the query. We quantify the precision of a query using
 291 the R-precision p_R , which is the precision at R-th position in the ranking of results for a query that has R
 292 relevant documents (in this case, R=10):

$$p_R = \frac{|\{\text{relevant documents}\} \cap \{\text{first 10 retrieved}\}|}{10} \quad (8)$$

293 and averaged p_R over all possible queries (n=100) in the test dataset to obtain a measure for each
 294 algorithm.

3.2 DESCRIPTIVE STATISTICS

295 Figures 3,4,5,6 and 7 display precision scores, color-coded from blue (low, < 70%) to red (high, > 85%),
 296 for all computational models based, resp., on time-series, frequency-series, rate-series, scale-series and
 297 on the non-series, vector approach. We give here descriptive statistics in each of these five approaches. We
 298 then use inferential statistics on the complete dataset to address transversal computational and biological
 299 questions, in the next section.

300 Among models that treat signals as a temporal series of features ($T>*$, Figure 3), those who incor-
 301 porate frequency as one of the dimensions of the feature space tend to perform best regardless of the
 302 algorithms (DP, GMM, PCA) used to compare the series. There is little advantage if any to add rates
 303 ($T>F, R$: precision $M=0.80$, $SD=0.05$, $\text{max}=0.85$) or scales ($T>F, S$: $M=0.83$, $SD=0.07$, $\text{max}=0.88$)
 304 to frequency only ($T>F$: $M=0.83$, $SD=0.08$, $\text{max}=0.89$). Summarizing F out of the feature space is larg-
 305 ely detrimental to precision: rates and scales alone are not effective if not linked to what frequency
 306 theyre operating on. $T>R$ ($M=0.73$, $SD=0.07$, $\text{max}=0.77$), $T>S$ ($M=0.64$, $SD=0.06$, $\text{max}=0.68$) and
 307 $T>R, S$ ($M=0.76$, $SD=0.07$, $\text{max}=0.80$) are all suboptimal. Among temporal series, models that compare
 308 series with GMMs ($M=0.80, SD=0.07$) tend to perform better than those who do with alignment distances
 309 ($M=0.74, SD=0.09$). Whether PCA is used or not has no effect on GMM accuracy, but it has for alignment
 310 distances: PCA: $M=0.67, SD=0.07$; no PCA: $M=0.79, SD=0.06$.

311 For models treating data as a frequency series ($F>*$, Figure 4), the inclusion of rates and scales in the
 312 feature vector improves precision: frequency series taking values conjunctly in rate and scale ($F>S, R$:
 313 $M=0.83, SD=0.07, \text{max}=0.91$) are better than independantly ($F>S$: $M=0.73, SD=0.11, \text{max}=0.89$; $F>R$:

314 $M=0.76$, $SD=0.03$, $\max=0.78$). Interestingly, frequency series in rate-scale space are more effective than
 315 time-series in rate-scale ($T>R$, S : $M=0.76$, $SD=0.07$, $\max=0.80$). There was no effect among frequency
 316 series of comparing with GMMs or alignment distance. As for temporal series, PCA had no effect on
 317 GMM algorithms, but was detrimental to alignment distances (PCA: $M=0.70$, $SD=0.06$; no PCA: $M=0.86$,
 318 $SD=0.06$).

319 For models treating data as a rate series ($R>*$, Figure 5) the frequency dimension is the single most
 320 effective contribution to the feature space ($R>F$: $M=0.79$, $SD=0.10$, $\max=0.86$; $R>S$: $M=0.71$, $SD=0.14$,
 321 $\max=0.84$). The conjunct use of F and S improves performance even further: $R>F, S$: $M=0.84$, $SD=0.03$,
 322 $\max=0.86$. The performance of $R>F, S$ is in same range as $T>F, S$ ($M=0.83$, $SD=0.07$, $\max=0.88$)
 323 and $T>F$ ($M=0.83$, $SD=0.08$, $\max=0.89$). There was no effect among rate series of using either GMMs
 324 or alignment distances (GMM: $M=0.77$, $SD=0.10$ vs DP: $M=0.77$, $SD=0.11$). As above, there was no
 325 effect of PCA on GMM performance (PCA: $M=0.77$, $SD=0.11$; no PCA: $M=0.77$, $SD=0.11$), but it was
 326 detrimental to alignment distances: PCA: $M=0.71$, $SD=0.14$; no PCA: $M=0.84$, $SD=0.03$.

327 Scale-series ($S>*$, Figure 6) in frequency space ($S>F$: $M=0.80$, $SD=0.04$, $\max=0.83$) are better than in
 328 rate space ($S>R$, $M=0.70$, $SD=0.04$, $\max=0.74$), and only marginally improved by combining rate and
 329 frequency ($S>FR$, $M=0.82$, $SD=0.03$, $\max=0.83$). For rate series, GMMs tend to be more effective than
 330 alignment distances (GMM: $M=0.80$, $SD=0.05$; DP: $M=0.75$, $SD=0.07$). As above, there was no effect
 331 of PCA on GMM accuracy, and a detrimental effect of PCA on alignment distances (PCA: $M=0.72$, $SD=$
 332 0.06 ; no PCA: $M=0.78$, $SD=0.08$).

333 Finally, models which did not treat data as a series, but rather as a vector data (Figure 7) performed
 334 generally worse ($M=0.68$, $SD=0.18$) than models treating data as series ($M=0.77$, $SD=0.08$). There was
 335 no clear advantage to any conjunction of dimensions for these models. Euclidean distances were more
 336 effective ($M=0.71$, $SD=0.11$) than kernel distances ($M=0.65$, $SD=0.23$). PCA had no strong effect on
 337 the former (PCA: $M=0.72$, $SD=0.10$; no PCA: $M=0.68$, $SD=0.14$) but was crucial to the latter (PCA:
 338 $M=0.73$, $SD=0.16$; no PCA: $M=0.45$, $SD=0.26$).

3.3 FIVE COMPUTATIONAL AND BIOLOGICAL QUESTIONS

339 We use here inference statistics to show how this set of precision scores can be used to give insights
 340 into questions related to computational and biological audio systems. In all the following, performance
 341 differences between sets of algorithms were tested with one-factor ANOVAs on the R-precision values,
 342 using various algorithmic properties as a between-subject factor.

343 1. Is PCA-based dimensionality reduction a good idea with STRFs?

344
 345 PCA dimensionality reduction was tested both for series (with GMM and alignment distances) and
 346 for non-series models (with euclidean and kernel distances). Its effect on precision was surprisingly
 347 algorithm-dependent. For series models based on GMM modeling, PCA had no statistical effect on
 348 performance as tested by ANOVA: $F(1, 14)=.00001$, $p=.99$. However, using PCA was significantly
 349 detrimental when series were compared with alignment distances: $F(1, 14)=46.932$, $p=.00001$, with
 350 a 11% drop of R-precision (PCA: $M=0.70$, $SD=0.08$; no PCA: $M=0.81$, $SD=0.06$). Similarly, for
 351 non-series models, PCA had no effect on euclidean distance: $F(1, 21)=.49$, $p=.48$ (PCA: $M=0.72$,
 352 $SD=0.10$; no PCA: $M=0.68$, $SD=0.14$), but it was crucial to the good performance of kernel distan-
 353 ces: $F(1, 21)=9.63$, $p=.005$, with a 28% increase of R-precision (PCA: $M=0.73$, $SD=0.16$; no PCA:
 354 $M=0.45$, $SD=0.26$).

355 From a computational point of view, such mixed evidence does not conform to pattern-recognition
 356 intuition: data-driven dimensionality reduction is a standard processing stage after feature extraction
 357 (Müller et al., 2011) and efficient coding strategies are often directly incorporated in features them-
 358 selves (e.g. discrete cosine transform in the MFCC algorithm - Logan and Salomon (2001)). The
 359 detrimental impact of PCA on alignment distances may be a consequence of the whitening part of

360 the algorithm, which balances variance in all dimensions and does not not preserve the angles/cosine
 361 distances between frame vectors; whitening has no predicted consequence on GMMs, the covariance
 362 matrices of which can scale to compensate.

363 From a biological point of view, that PCA-like processing should be of little effect if applied to
 364 STRF suggests, first, that the STRF representation extracted by A1 neurons is already the result of
 365 efficient coding. This confirms previous findings that codewords learned with sparse coding strate-
 366 gies over speech and musical signals loosely correspond to the STRFs elicited with laboratory stimuli
 367 (Klein et al., 2003). Second, this suggests that subsequent cortical processing that operates on the
 368 STRF layer of A1 does not so much generate generic and efficient representations based on STRF,
 369 but perhaps rather act as an associative level that groups distributed STRF activations into interme-
 370 diate and increasingly specific representations - eventually resulting in specializations such as the
 371 lateral distinctions between fast and slow features of speech prosody in the superior temporal gyri
 372 (Schirmer and Kotz, 2006).
 373

374 2. Are we right to think in time (-series)? 375

376 All algorithms considered, models than treat signals as a series of either T,F,R or S tend to per-
 377 form better ($M=0.77$, $SD=0.08$) than models that are solely based on summary statistics ($M=0.68$,
 378 $SD=0.18$), $F(1, 108)=13.04$, $p=.00046$. However, among series, there was strikingly no performance
 379 advantage to any type of series: $F(3, 60)=.02$, $p=.99$ (T-series: $M=0.77$, $SD= 0.08$; F-series: $M=0.77$,
 380 $SD= 0.08$; R-series: $M=0.78$, $SD= 0.10$; S-series: $M=0.77$, $SD= 0.06$). In particular, there was no
 381 intrinsic advantage to the traditional approach of grouping features by temporal windows. Further,
 382 the best results obtained in this study were with a frequency series ($F>R, S$ with DTW).

383 From a computational point of view, this pattern is in stark contrast with the vast majority of audio
 384 pattern recognition algorithms that model signals as temporal series. A wealth of recent research
 385 focuses on what model best accounts for the temporal dynamics of such data, comparing statistical
 386 mixtures over time (Aucouturier and Pachet, 2007a) with e.g. Markov models (Flexer et al., 2005),
 387 explicit dynamical models (Lagrange, 2010) or multi-scale pooling (Hamel et al., 2011). Our results
 388 suggest that collapsing the temporal dimension does not necessarily lead to reduced performance;
 389 what seems to matter rather is to group feature observations according to *any* physical dimensions of
 390 the signal, e.g. frequency. Such alternative, non-temporal paradigms remain mostly unexplored in the
 391 audio pattern recognition community.

392 From a biological point of view, this pattern suggests that, for the task studied here, structured
 393 temporal representations are not a computational requirement. This is compatible with recent experi-
 394 mental evidence showing that at least part of the human processing of sound textures relies only on
 395 summary statistics (McDermott et al., 2013; Nelken and de Cheveigné, 2013).
 396

397 3. Are STRF representations more effective than time-frequency representations? 398

399 The results of Patil et al. (2012) were taken as a proof-of-concept that STRF representations are
 400 more effective in simulating human similarity judgements that representations based only on time and
 401 frequency. Their demonstration is based on a single algorithmic strategy to calculate similarities from
 402 STRFs. Our data, based on more than a hundred alternative algorithms, provides more contrasted
 403 evidence. In order to link performance to the conjunction of dimensions used in the models' feature
 404 space, we performed a one-factor ANOVA using a 6-level dimension factor: R,S,R,F-S,F-R and F-
 405 S-R. For series data (regardless of the time,frequency, rate or scale basis for the series), there was a
 406 main effect of dimension: $F(6, 55)=4.85$, $p=.0005$. Posthoc difference (Fisher LSD) revealed that both
 407 $*>R$ and $*>S$ feature spaces are significantly less effective than $*>F$, $*>RS$ and any combination of
 408 F with S,R. (Figure 8). For vector data, there was no main effect of dimension: $F(6, 37)=.51$, $p=0.79$.
 409 In other words, processing the rate and scale dimensions only benefits algorithms which also process
 410 frequency, and is detrimental otherwise. Moreover, algorithms which only process frequency are no
 411 less effective than algorithms which also process rate and scale.

412 It is still possible that, because of their sparser nature, scale and rate representations allow faster,
413 rather than more effective, responses than the more redundant time-frequency representations, as do
414 efficient coding strategies in the visual cortex (Serre et al., 2007). Second, such representations may
415 also be more learnable, e.g. requiring fewer training instances to build generalizable sensory repre-
416 sentations.

417

418 4. Does the topology of neuronal responses determine cortical algorithms?

419

420 The orderly mapping in cortical space of characteristic neuronal responses, such as the tonotopical
421 map of characteristic frequencies, plausibly reflects a computational need to process several areas
422 of the corresponding dimensions conjunctly (Eggermont, 2010). Performance data for the group
423 of algorithms investigated in this study seems to corroborate this intuition. First, the most efficient
424 models for our task tend to operate primarily on frequency: rate and scale data is only effective if
425 treated conjunctly with frequency, and it can be summarized out to little cost as long as the frequency
426 axis is maintained (Figure 8). Second, in F-R-S models, it was found more effective to reduce the
427 dimensionality of the R-S space while preserving the F axis, rather than reducing the dimension of
428 the conjunct F-R-S space (Figure 7). Third, the best performing algorithm found here treats data as
429 a frequency series, i.e. a series of successive R-S maps measured along the tonotopical axis (F>RS).
430 Finally, models that put similar emphasis on R and S rather than F are typically low performers, and
431 processing either R and S appears to be relatively inter-changeable. This computational behaviour
432 therefore fully supports a structurative role of the frequency dimension in cortical representations of
433 sound, and is in accordance with the fact that no rate and scale gradients have been observed to date
434 in the mammalian auditory cortex, even within each isofrequency lamina (Atencio and Schreiner,
435 2010).

436

437 5. What are the cortical equivalents of the series and vector approaches, and why is the former 438 more effective?

439

440 Contrary to the vector approach, series models proceed by grouping feature observations in succes-
441 sive (if time-based) or simultaneous (if frequency-, rate- or scale-based) categories, providing a
442 two-layer representation of the data. All algorithms considered, such representations ($*>*$) appear
443 more effective ($M=0.77$, $SD=0.08$) than those which treat STRF data as a single unstructured ensemble
444 ($M=0.68$, $SD=0.18$), $F(1, 108)=13.0$, $p=.0004$. While this computational observation is in some
445 accordance with the tonotopic structure of the auditory cortex, it is unclear why it should be more
446 effective. First, grouping STRF activation data into several categories that can be considered simul-
447 taneously may be a simple and agnostic way to represent heterogeneous stimuli, e.g. stimuli that are
448 slowly-changing in the low-frequency band while rapidly-changing in the high-frequency band (Lu
449 et al., 2001). Second, such structured representations may provide a more compact code for storing
450 exemplars in memory (McDermott et al., 2013). This may further indicate that the memory struc-
451 tures that store sensory traces for e.g. exemplar comparison, are organized in the same structured
452 laminae as the sensory structures - see also Weinberger (2004).

453

454 Additionally, to process such series data, there was no strong difference between the GMM and
455 DP approaches: GMMs yielded marginally superior performance for time- and scale-series and were
456 equivalent to DP for frequency- and rate-series. This computational observation suggests that, while
457 it is important to group data into categories, there is no strong requirement to process the differ-
458 ences/transitions from one category to the next (as done by DP); rather, it is the variability among
categories (as modeled by GMMs) that seems most important to account for.

4 DISCUSSION

459 Meta-analysis of the precision values in the above case-study revealed that the most effective represen-
460 tations to retrieve the categorical structure of the corpus should (1) preserve information about center
461 frequency rather than averaging over this dimension, and (2) process the output as a series, e.g. with
462 respect to this center-frequency dimension and not necessarily to time. These two computational trends
463 are in interesting accordance with the tonotopical organisation of STRFs in A1 as well as recent findings
464 on texture discrimination by summary statistics (McDermott et al., 2013; Nelken and de Cheveigné,
465 2013). More generally, this suggests that meta-analysis over a space of computational models (possibly
466 explored exhaustively) can generate insights that would otherwise be overlooked in a field where cur-
467 rent results are scattered, having been developed with different analytical models, fitting methods and
468 datasets.

469 In particular, this work extends the work of Patil et al. (2012) by testing, on a new dataset, which
470 of its design choices are most computationally important. Their approach can be classified as non-series
471 (summarize T), with PCA on the 30,976-dimension F-R-S space, then a kernel distance (the top-most path
472 in Figure 7). On our dataset, this approach lead to a R-precision of 70%. Among the 105 other models
473 tested in the present study, some were found more effective for our specific task: if keeping with non-series
474 models, a simple improvement is to apply PCA only on the 22-dimension R-S space while preserving
475 the 128 dimensions of the frequency axis (88% R-precision). More systematically, better results were
476 achieved when considering data as a series rather than a vector. For instance, modeling the time dimension
477 as a GMM rather than a one-point average, otherwise keeping the same feature space and PCA strategy
478 yields an improvement of 10% (79.3%, top-most path in Figure 3). The original finding was taken to
479 indicate that the modulation features (rates and scales) extracted by STRFs are crucial to the representation
480 of sound textures, and that the simpler, and more traditionally used, time-frequency representations are
481 insufficient both from a computational and biological point of view. Data from the above case-study,
482 based on more than a hundred alternative algorithms, provides more contrasted evidence: processing
483 the rate and scale dimensions only benefits algorithms which also process frequency, and is detrimental
484 otherwise. Moreover, algorithms which only process frequency were no less effective, for the task and
485 corpus of the present case-study, than algorithms which also process rate and scale.

486 One should not, however, overestimate the biological relevance of the patterns mined from the case-
487 study presented here. It is well-known that pattern recognition methods (both in terms of feature
488 representation, classifiers or distance metrics) depend critically on the structure of the data itself, e.g.
489 how many exemplars and how much variance in each category, as well as how much overlap between
490 categories (see e.g. Lagrange et al. (2014)). The corpus used here results of a compromise between the
491 need to reflect the full range of natural sounds (e.g. bird songs and water textures) and the need to include
492 overlapping categories (e.g. pouring water and waterways). However, it remains difficult to assess the
493 extent conclusions from the present case-study may simply reflect the specific structure of the sounds
494 and task used in the analysis. For instance, the importance of preserving center frequency evidenced in
495 the present study may suggest that the specific environmental sound categories used in the test corpus
496 were simply more easily separable with frequency information than with temporal cues. It is possible that
497 other types of stimuli with more elaborate temporal structure than environmental textures, e.g. speech or
498 polyphonic music, require more structured time representations. Similarly, the classification task used in
499 the present case-study does not reflect the full range of computations performed by biological systems on
500 acoustic input. It is possible that other types of computations (e.g. similarity judgements) or other aspects
501 of these computations (e.g. processing speed, representation compactness) could benefit from the addi-
502 tional representational power of rate and scale dimensions more than the task evaluated here. The trends
503 identified here should therefore be confirmed on a larger sound dataset with more exemplars per category
504 (Giannoulis et al., 2013) or, better yet, meta-analysed across multiple separate datasets (Misdariis et al.,
505 2010).

506 Finally, one should also note that the STRF model used in this study is linear, while auditory cortical
507 neurons have known non-linear characteristics. In particular, neurophysiological studies have suggested

508 that a non-linear spike threshold can impact neural coding properties (Escabí et al., 2005). Further work
509 should incorporate such non-linearities in the representations explored here, both to increase the bio-
510 logical relevance of the meta-analysis and to better understand the added computational value of these
511 mechanisms compared to simpler linear representations.

DISCLOSURE/CONFLICT-OF-INTEREST STATEMENT

512 The authors declare that the research was conducted in the absence of any commercial or financial
513 relationships that could be construed as a potential conflict of interest.

AUTHOR CONTRIBUTIONS

514 EH and JJA contributed equally to designing and implementing the experiments, analysing data and
515 drafting the present article. Author order was determined by seniority.

ACKNOWLEDGEMENT

516 The authors thank Mounya El Hilali and Shihab Shamma for kindly providing additional information on
517 the work of Patil et al. (2012). The authors also thank Frédéric Theunissen and Konrad Kording for their
518 comments on earlier versions of the manuscript.

REFERENCES

- 519 Asari, H. and Zador, A. M. (2009), Long-lasting context dependence constrains neural encoding models
520 in rodent auditory cortex, *Journal of neurophysiology*, 102, 5, 2638–2656
- 521 Atencio, C. and Schreiner, C. (2010), Columnar connectivity and laminar processing in cat primary
522 auditory cortex, *PLoS One*
- 523 Aucouturier, J. and Pachet, F. (2004), Improving timbre similarity: How high's the sky?, *Journal of*
524 *Negative Results in Speech and Audio Sciences*, 1(1)
- 525 Aucouturier, J.-J. and Pachet, F. (2007a), The bag-of-frame approach to audio pattern recognition: a
526 sufficient model for urban soundscapes but not for polyphonic music, *Journal of the Acoustical Society*
527 *of America*, 122(2), 881–891
- 528 Aucouturier, J.-J. and Pachet, F. (2007b), The influence of polyphony on the dynamical modelling of
529 musical timbre, *Pattern Recognition Letters*, 28, 5, 654–661
- 530 Baumann, S., Griffiths, T., Sun, L., Petkov, C., Thiele, A., and Rees, A. (2011), Orthogonal representation
531 of sound dimensions in the primate midbrain, *Nature Neuroscience*, 14
- 532 Bishop, C. M. and Nasrabadi, N. M. (2006), *Pattern recognition and machine learning* (New York:
533 springer)
- 534 Chi, T., Ru, P., and Shamma, S. (2005), Multiresolution spectrotemporal analysis of complex sounds,
535 *Journal of the Acoustical Society of America*, 118, 887–906
- 536 Christianson, G., Sahani, M., and Linden, J. (2008), The consequences of response non-linearities for
537 interpretation of spectrotemporal receptive fields, *Journal of Neuroscience*, 28, 446–455
- 538 David, S. V. and Shamma, S. A. (2013), Integration over multiple timescales in primary auditory cortex,
539 *The Journal of Neuroscience*, 33, 49, 19154–19166
- 540 Eggermont, J. J. (2010), The auditory cortex: the final frontier, in R. Meddis, E. Lopez-Poveda, A. popper,
541 and R. Fay, eds., *Computational Models of the Auditory System*. Springer Handbook of Auditory
542 Research 35 (New York: Springer), 97–127

- 543 Escabí, M. A., Nassiri, R., Miller, L. M., Schreiner, C. E., and Read, H. L. (2005), The contribution of
544 spike threshold to acoustic feature selectivity, spike information content, and information throughput,
545 *The Journal of neuroscience*, 25, 41, 9524–9534
- 546 Fishbach, A., Yeshurun, Y., and Nelken, I. (2003), Neural model for physiological responses to frequency
547 and amplitude transitions uncovers topographical order in the auditory cortex, *J. Neurophysiology*, 90,
548 2303–2323
- 549 Flexer, A., Pampalk, E., and Widmer, G. (2005), Hidden markov models for spectral similarity of songs,
550 in Proc. of the 8th Int. Conference on Digital Audio Effects (DAFx), Madrid, Spain
- 551 Gehr, D., Komiya, H., and Eggermont, J. (2000), Neuronal responses in cat primary auditory cortex to
552 natural and altered species-specific calls, *Hearing Research*, 150, 27–42
- 553 Giannoulis, D., Benetos, E., Stowell, D., Rossignol, M., Lagrange, M., and Plumbley, M. (2013), Dete-
554 ction and classification of acoustic scenes and events: An ieeea asp challenge, in Proceedings of the
555 2013 IEEE Workshop on Applications of Signal Processing to Audio and Acoustics (WASPAA 2013)
- 556 Gourévitch, B., Noreña, A., Shaw, G., and Eggermont, J. (2009), Spectro-temporal receptive fields in
557 anesthetized cat primary auditory cortex are context dependent, *Cerebral Cortex*, 19(6), 1448–1461
- 558 Halko, N., Martinsson, P.-G., and Tropp, J. A. (2011), Finding structure with randomness: Probabilistic
559 algorithms for constructing approximate matrix decompositions, *SIAM review*, 53, 2, 217–288
- 560 Hamel, P., Lemieux, S., Bengio, Y., and Eck, D. (2011), Temporal pooling and multiscale learning
561 for automatic annotation and ranking of music audio., in Proc. International Conference on Music
562 Information Retrieval, 729–734
- 563 Kim, G. and Doupe, A. (2011), Organized representation of spectrotemporal features in songbird auditory
564 forebrain, *The Journal of Neuroscience*, 31(47)
- 565 Klein, D., Konig, P., and Kording, K. (2003), Sparse spectrotemporal coding of sounds, *EURASIP J.*
566 *Applied Signal Processing*, 7
- 567 Lagrange, M. (2010), Explicit modeling of temporal dynamics within musical signals for acoustical unit
568 formation and similarity, *Pattern Recognition Letters*
- 569 Lagrange, M., Aucouturier, J., and Defreville, B. (2014), The bag-of-frame approach: a not-so sufficient
570 model for urban soundscapes after all, *submitted*
- 571 Logan, B. and Salomon, A. (2001), A music-similarity function based on signal analysis, *International*
572 *Conference on Multimedia and Expo*
- 573 Lu, T., Liang, L., and Wang, X. (2001), Temporal and rate representations of time-varying signals in the
574 auditory cortex of awake primates, *Nature Neuroscience*, 4(11)
- 575 McDermott, J., Schemistch, M., and Simoncelli, E. (2013), Summary statistics in auditory perception,
576 *Nature Neuroscience*, 16(4)
- 577 Misdariis, N., Minard, A., Susini, P., Lemaitre, G., McAdams, S., and Parizet, E. (2010), Environmental
578 sound perception: Metadescription and modeling based on independent primary studies, *EURASIP*
579 *Journal on Audio, Speech, and Music Processing*
- 580 Müller, M., Ellis, D. P. W., Klapuri, A., and Richard, G. (2011), Signal processing for music analysis,
581 *IEEE Journal of Selected Topics in Signal Processing*, 5(6), 1088–1110
- 582 Nelken, I. and de Cheveigné, A. (2013), An ear for statistics, *Nature Neuroscience*, 16, 381–382
- 583 Orio, N. (2006), Music retrieval: a tutorial and review, *Found. Trends Information Retrieval*, 1(1)
- 584 Pampalk, E. (2006), Audio-based music similarity and retrieval: combining a spectral similarity model
585 with information extracted from fluctuation patterns, in Proceedings of the ISMIR International
586 Conference on Music Information Retrieval (ISMIR'06), Vienna, Austria
- 587 Patil, K., Pressnitzer, D., Shamma, S., and Elhilali, M. (2012), Music in our ears: The biological bases of
588 musical timbre perception, *PLOS Computational Biology*, 8(11)
- 589 Peeters, G., La Burthe, A., and Rodet, X. (2002), Toward automatic music audio summary generation
590 from signal analysis, in In Proc. International Conference on Music Information Retrieval, 94–100
- 591 Schirmer, A. and Kotz, S. (2006), Beyond the right hemisphere: Brain mechanisms mediating vocal
592 emotional processing, *Trends in Cognitive Sciences*, 10, 24–30
- 593 Schreiner, C., Read, H., and Sutter, M. (2000), Modular organization of frequency integration in primary
594 auditory cortex, *Annual Review of Neuroscience*, 23

- 595 Serre, T., Wolf, L., Bileschi, S., Riesenhuber, M., and Poggio, T. (2007), Object recognition with cortex-
596 like mechanisms, *IEEE Transactions on Pattern Analysis and Machine Intelligence*, 29(3), 411–426
597 Sethares, W. A. and Staley, T. (1999), The periodicity transform, *IEEE Trans. Signal Processing*, 47(11)
598 Ulanovsky, N., Las, L., and Nelken, I. (2003), Processing of low-probability sounds by cortical neurons,
599 *Nature neuroscience*, 6, 4, 391–398
600 Weinberger, N. M. (2004), Specific long-term memory traces in primary auditory cortex, *Nature Reviews*
601 *Neuroscience*, 5(4), 279–290

FIGURES

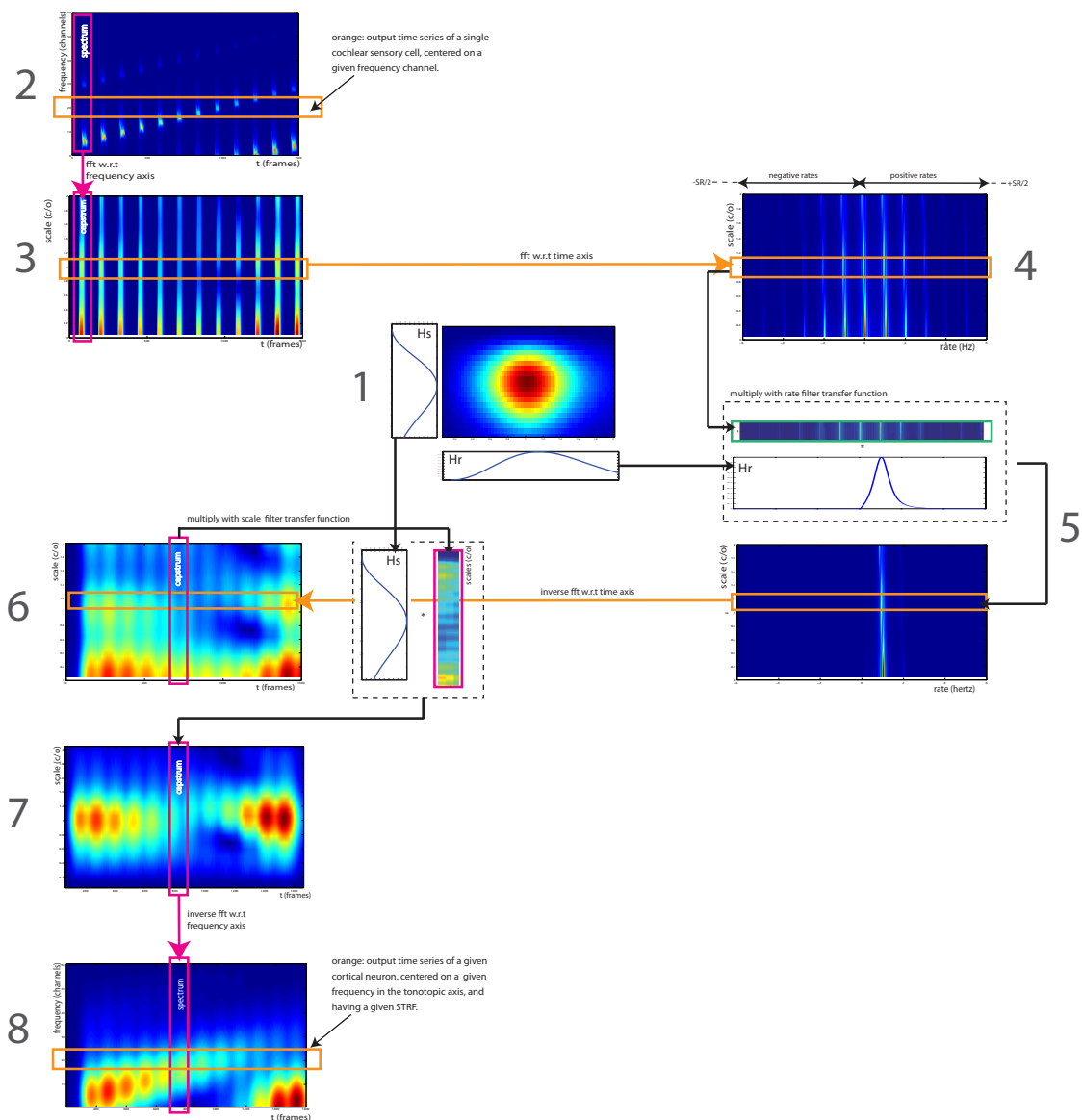


Figure 1. Signal processing workflow of the STRF model, as implemented by Patil et al. (2012). The STRF model simulates the cortical processing occurring in the auditory thalamus and cortex. It processes the output of the cochlea - represented here by an auditory spectrogram in log frequency ($SR=24$ channels per octave) vs time ($SR=125\text{Hz}$), using a multitude of cortical neuron each tuned on a frequency (in Hz), a modulation w.r.t time (a rate, in Hz) and w.r.t. frequency (a scale, in cycles/octave). We take here the example of a 12-second series of 12 Shepards tones, i.e. a periodicity of 1Hz in time and 1 harmonic partial/octave in frequency, processed by a STRF centered on rate = 1Hz and scale = 1 c/o (1). In the input representation (2), each frequency slice (orange) corresponds to the output time series of a single cochlear sensory cell, centered on a given frequency channel. In the output representation (8), each frequency slice (orange) corresponds to the output of a single cortical neuron, centered on a given frequency on the tonotopic axis, and having a given STRF. The full model (not shown here) has hundreds of STRFs (e.g. 22 rates * 11 scales = 242), thus thousands of neurons (e.g. 128 freqs * 242 STRFs = 30,976).

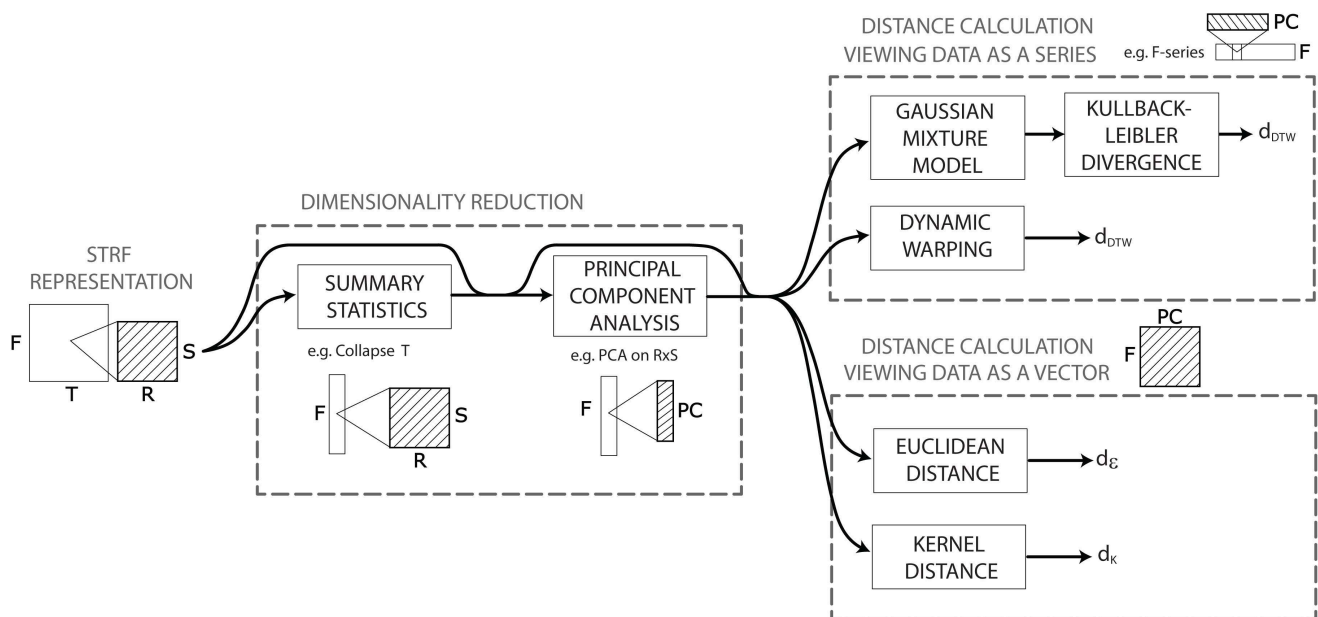
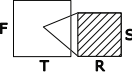
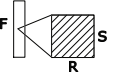
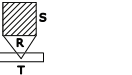
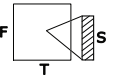
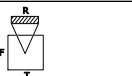
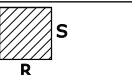

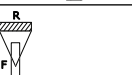
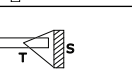
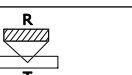

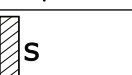


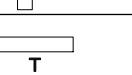


Figure 2. Pattern recognition workflow of the distance calculation based on the STRF model. The STRF model provides a high-dimensional representation upon which we construct more than a hundred algorithmic ways to compute acoustic dissimilarities between pairs of audio signals. All these algorithms obey to a general pattern recognition workflow consisting of a dimensionality reduction stage, followed by a distance calculation stage. The dimensionality reduction stage aims to reduce the dimension ($d=30,976 \times \text{time}$) of the STRF representation to make it more computationally suitable to the algorithms operating in the distance calculation stage - we use here summary statistics and/or principal component analysis (PCA). The distance computation stage differs on whether it treats a signal's STRF data as a single multidimensional point in a vector space, or as a series of points. In the former case, we use either the euclidean distance or the gaussian kernel distance. In the latter case, we use either Kullback-Leibler divergence between gaussian mixture models of the series, or dynamic programming/dynamic time warping.

Table 1. All possible combinations of reduced representations derived from the STRF model. Some of these reduced representations are conceptually similar to signal representations that are used in the audio pattern recognition community. We name here some which we could identify; the other unnamed constructs listed here are germane to the present study to the best of our knowledge. The choice of which distance calculation algorithm to apply on each representation depends on whether it can be as a single vector (V) or as a series in time (T), frequency (F), rate (R) or scale (S). For instance, representations in which the time dimension is preserved can only be considered as a time-series. Similarly, the combinations of dimensions that can be reduced with PCA depends on each representation. The table lists which processing is possible for each representation.

Dimensions	Summarize	in state-of-art as:	PCA possible on:	Processing as:				
				T	F	R	S	V
	\emptyset	STRF (Chi et al. , 2005)	FRS	✓				
	T	Average STRF maps (Patil et al. , 2012)	FR,FS,FRS		✓	✓	✓	✓
	F	?	RS	✓				
	R	?	FS	✓				
	S	?	FR	✓				
	T,F	?	R,S,RS			✓	✓	✓
	T,R	?	F,S,FS		✓		✓	✓
	T,S	Fluctuation patterns (Pampalk , 2006)	F,R,FR		✓	✓		✓
	F,R	MFCCs (Logan and Salomon , 2001)	S	✓				
	F,S	Modulation spectrum (Peeters et al. , 2002)	R	✓				
	R,S	Fourier spectrogram	F	✓				
	T,F,R	Average Cepstrum	S				✓	✓
	T,F,S	Periodicity transform (Sethares and Staley , 1999)	R			✓		✓
	T,R,S	Fourier spectrum	F		✓			✓
	F,R,S	Waveform	\emptyset	✓				

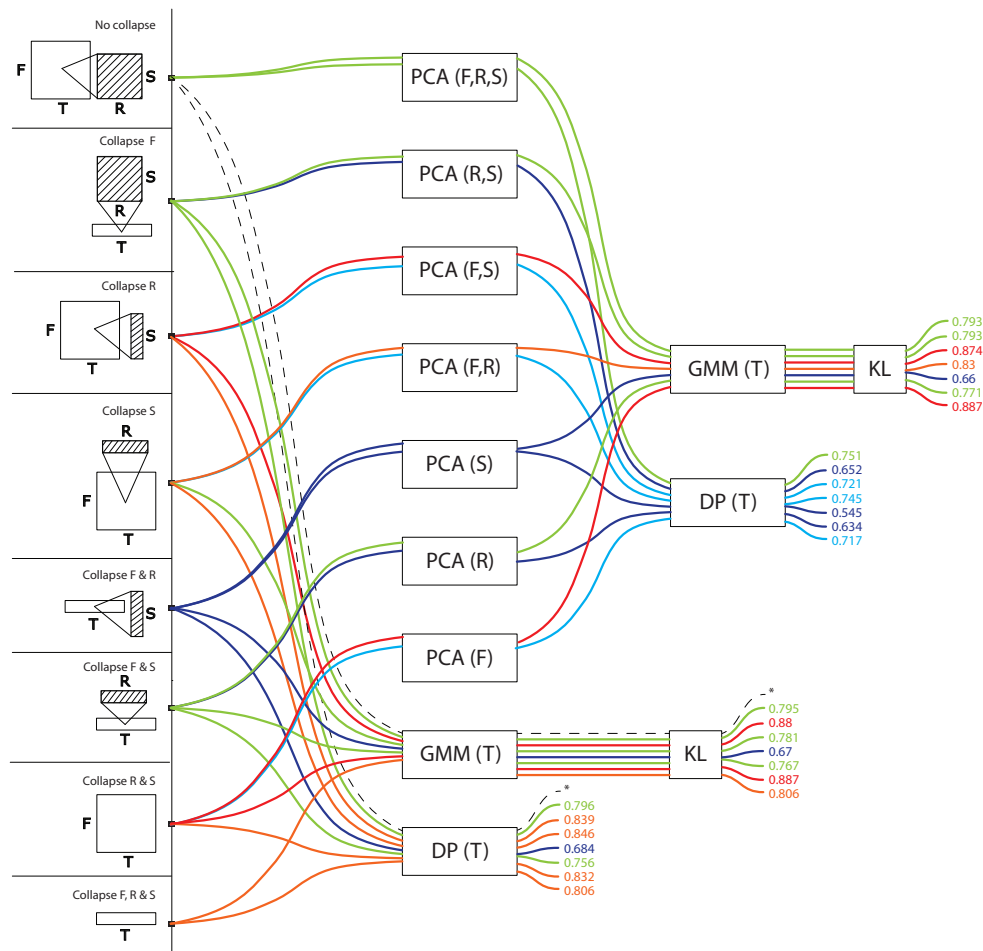


Figure 3. Precision values for all computational models based on temporal series. These models treat signals as a trajectory of features grouped by time window, taking values in a feature space consisting of frequency, rate and scale (or any subset thereof). Precisions are color-coded from blue (low, < 70%) to red (high, > 85%)

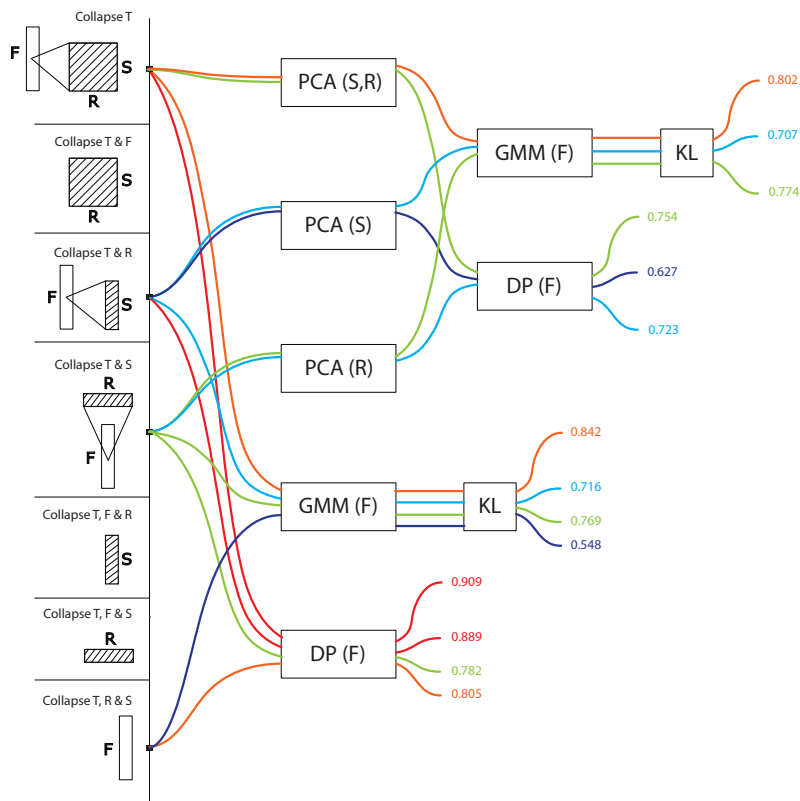


Figure 4. Precision values for all computational models based on frequency series. These models treat signals as a trajectory of values grouped by frequency, taking values in a feature space consisting of rates and scales (or any subset thereof). Precisions are color-coded from blue (low, < 70%) to red (high, > 85%)

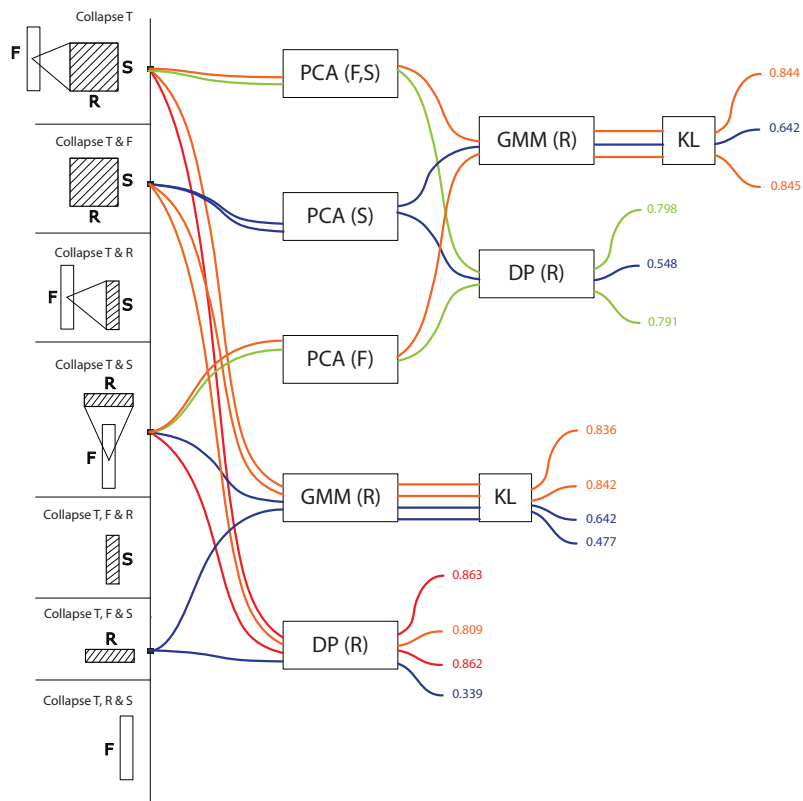


Figure 5. Precision values for all computational models based on rate series. These models treat signals as a trajectory of values grouped by rate, taking values in a feature space consisting of frequencies and scales (or any subset thereof). Precisions are color-coded from blue (low, < 70%) to red (high, > 85%)

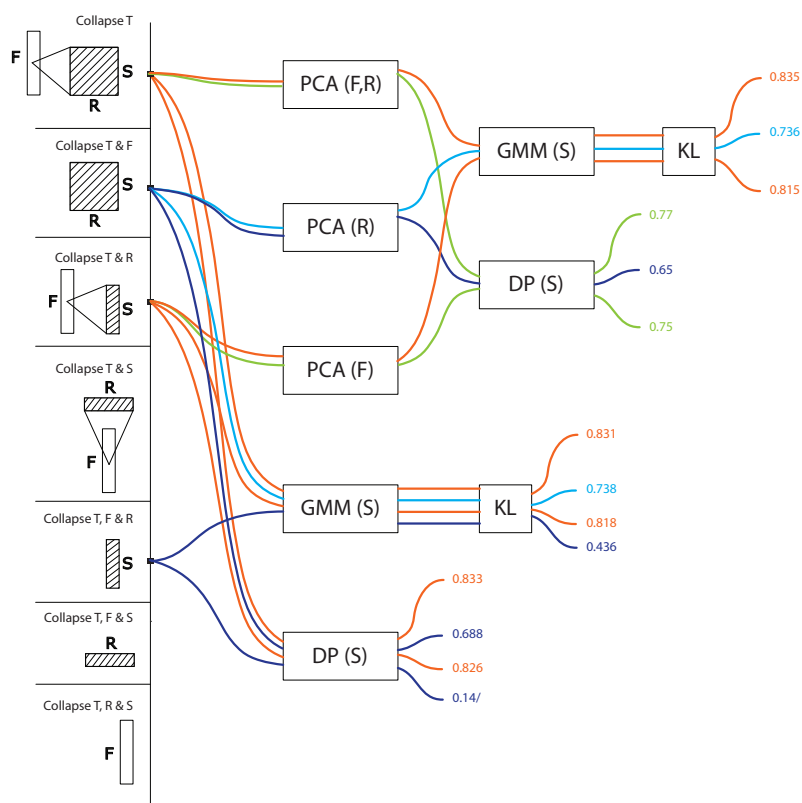


Figure 6. Precision values for all computational models based on scale series. These models treat signals as a trajectory of values grouped by scale, taking values in a feature space consisting of frequencies and rates (or any subset thereof). Precisions are color-coded from blue (low, < 70%) to red (high, > 85%)

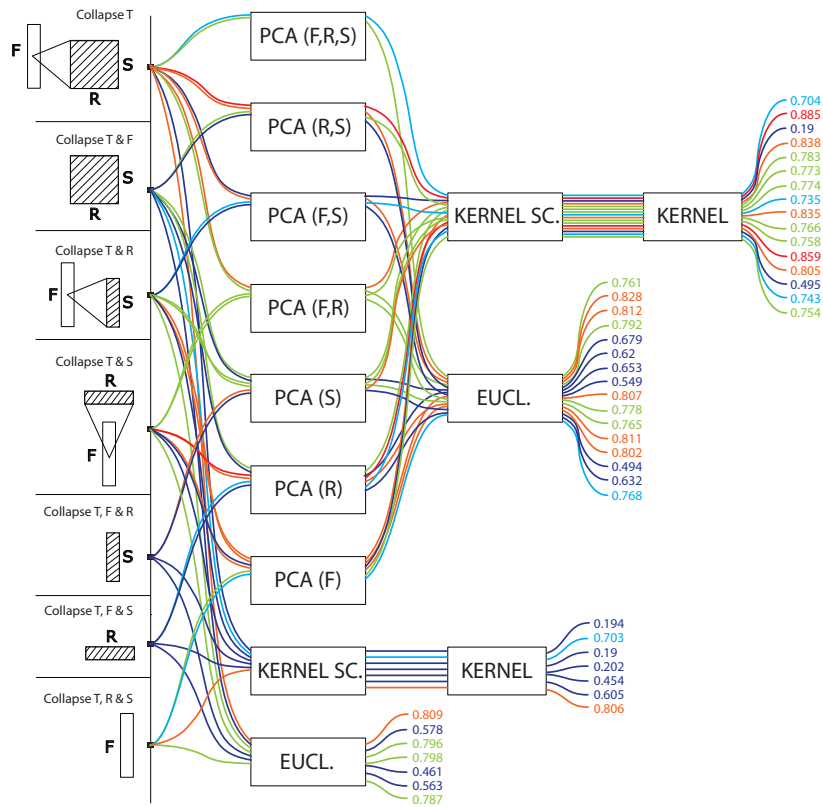


Figure 7. Precision values for all computational models based on vector data. These models do not treat any particular dimension as a series, but rather applied dimension reduction (namely, PCA) on various combinations of time, frequency, rate and scale, to yield a single high-dimensional vector representation for each signal. Vectors are compared to one another using euclidean or kernel distances. Precisions are color-coded from blue (low, < 70%) to red (high, > 85%)

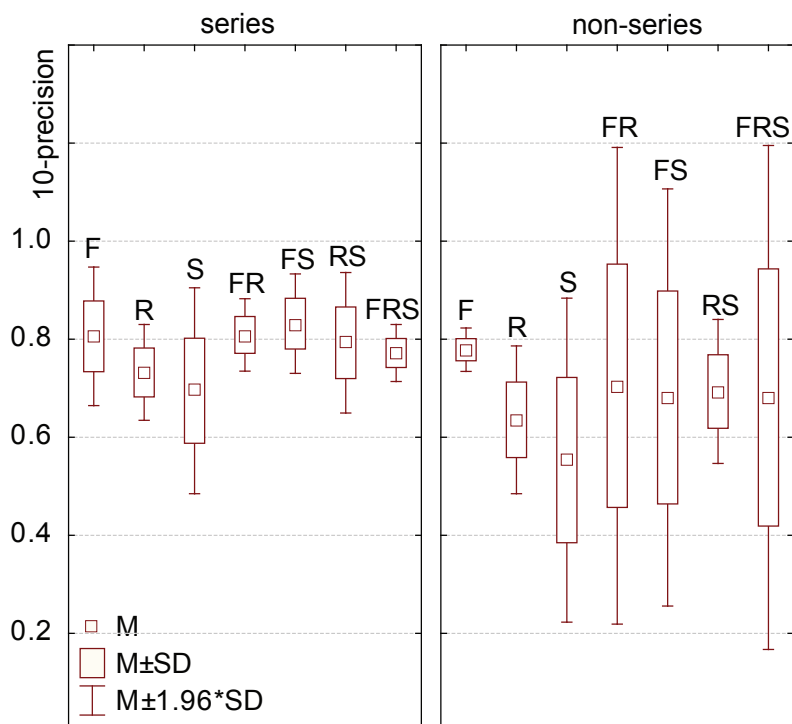


Figure 8. Model performance depending on the dimensions embedded in its feature space. For series data (regardless of the time, frequency, rate or scale basis for the series), feature spaces consisting of frequency, frequency+rate and frequency+scale were the most effective. Feature spaces consisting of only rates or scales (not in combination with frequency) were significantly less effective. For non-series data, differences were in the same trend but non-significant.